THE JOURNAL OF BIOLOGICAL CHEMISTRY VOL. 292, NO. 14, pp. 6014–6026, April 7, 2017

SERINC5 protein inhibits HIV-1 fusion pore formation by promoting functional inactivation of envelope glycoproteins

Received for publication, January 19, 2017, and in revised form, February 7, 2017 Published, JBC Papers in Press, February 8, 2017, DOI 10.1074/jbc.M117.777714

Chetan Sood[‡1], **Mariana Marin**[‡1], **Ajit Chande**[§], **Massimo Pizzato**[§], **and Gregory B. Melikyan**[‡2]

From the [‡]*Department of Pediatrics, Emory University, Atlanta, Georgia 30322 and the* [§]*Centre for Integrative Biology, University of Trento, 38123 Trento, Italy*

Edited by Charles E. Samuel

The host proteins, SERINC3 and SERINC5, have been recently shown to incorporate into HIV-1 particles and compromise their ability to fuse with target cells, an effect that is antagonized by the viral Nef protein. Envelope (Env) glycoproteins from different HIV-1 isolates exhibit a broad range of sensitivity to SERINC-mediated restriction, and the mechanism by which SERINCs interfere with HIV-1 fusion remains unclear. Here, we show that incorporation of SERINC5 into virions in the absence of Nef inhibits the formation of small fusion pores between viruses and cells. Strikingly, we found that SERINC5 promotes spontaneous functional inactivation of sensitive but not resistant Env glycoproteins. Although SERINC5-Env interaction was not detected by co-immunoprecipitation, incorporation of this protein enhanced the exposure of the conserved gp41 domains and sensitized the virus to neutralizing antibodies and gp41-derived inhibitory peptides. These results imply that SERINC5 restricts HIV-1 fusion at a step prior to small pore formation by selectively inactivating sensitive Env glycoproteins, likely through altering their conformation. The increased HIV-1 sensitivity to anti-gp41 antibodies and peptides suggests that SER5 also delays refolding of the remaining fusion-competent Env trimers.

It has long been recognized that Nef enhances the HIV-1 infectivity measured by a single cycle infection assay (1–8), but the underlying mechanism remained poorly understood. Nef has been reported to enhance an early step of HIV-1 entry upstream of reverse transcription (1, 2); however, researchers disagreed as to whether Nef incorporation promotes the HIV-1 fusion step (3–7, 9). Two recent papers have elucidated the infectivity-enhancing effect of Nef by showing that SERINC5 (SER5) and, to a lesser extent, SERINC3 expressed in infected cells incorporate into HIV-1 particles in the absence of Nef and potently inhibit infectivity of released virions (10, 11). The antiviral activity of SER5 is antagonized by HIV/simian immunodeficiency virus Nef and by the unrelated glycoGag protein of murine leukemia virus (MLV),[3] which are thought to diminish SER5 incorporation into virions by removing it from the plasma membrane (10, 11). The importance of SER5 as a restriction factor is strongly supported by the observation that the potency with which Nef antagonizes this protein correlates with the prevalence of primate lentiviruses in the wild (12).

Little is known about SER5, except that this multipass transmembrane protein appears to be involved in serine incorporation into lipids and promotion of phosphatidylserine (PS) and sphingomyelin biosynthesis (13). Virus-incorporated SER5 has been shown to inhibit HIV-1 fusion (10, 11), but the HIV-1 Env glycoproteins differ in their sensitivity to this factor, with the primary JRFL isolate being much less sensitive than the laboratory-adapted strains, such as NL4-3. Whereas MLV infection is also antagonized by SER5, fusion of HIV-1 particles pseudotyped with vesicular stomatitis virus (VSV)-G or Ebola virus glycoproteins is relatively resistant to this factor (10, 11, 14). In fact, Ebola pseudovirus infectivity has been reported to be enhanced by incorporation of SER5 (15).

Accumulating evidence implies that Nef is incapable of blocking SER5 incorporation into HIV-1 particles upon overexpression of this restriction factor (16, 17) but that Env itself is a major determinant of SER5 sensitivity (16). Specifically, the Nef/glycoGag dependence of HIV-1 infectivity (and thus its sensitivity to SER3/SER5) has been mapped to the gp120 V1/V2 loops (18), while a recent study revealed a critical role of the V3 loop in modulating the Env sensitivity to SER5 (16). New evidence also suggests that, in addition to its role in SER5 internalization from the plasma membrane, Nef antagonizes the activity of virus-incorporated SER5 by a cryptic mechanism (17).

Although the mechanism by which SER5 inhibits HIV-1 fusion is not understood, the observation that SER5 more potently blocks HIV-1 infection than fusion led to a model that this protein impairs the enlargement of the fusion pore and thereby the release of viral nucleocapsid (10, 11). Here, we investigated the effect of SER5 incorporated into HIV-1 particles on viral fusion in the absence of Nef. Functional virus-cell and cell-cell fusion assays and single virus imaging show that

This work was supported by National Institutes of Health Grant R01 GM054787 (to G. B. M.), FP7 Marie Curie Career Integration Grant 322130, and Caritro "Ricerca Biomedica" Grant 2013.0248 (to M. P.). The authors declare that they have no conflicts of interest with the contents of this article. The content is solely the responsibility of the authors and does not necessarily represent the official views of the National Institutes of Health.
This article was selected as one of our Editors' Picks.
This article contains supplemental Figs. S1–S6.
[1] Both authors contributed equally to this work.
[2] To whom correspondence should be addressed. Tel.: 404-727-4652; E-mail: gmeliki@emory.edu.

[3] The abbreviations used are: MLV, murine leukemia virus; PS, phosphatidylserine; VSV, vesicular stomatitis virus; FFWO, fusion-from-without; CPZ, chlorpromazine; MPER, membrane-proximal extracellular region; Env, envelope; FB, FluorBrite; FRAP, fluorescence recovery after photobleaching; HBSS, Hanks' balanced salt solution.

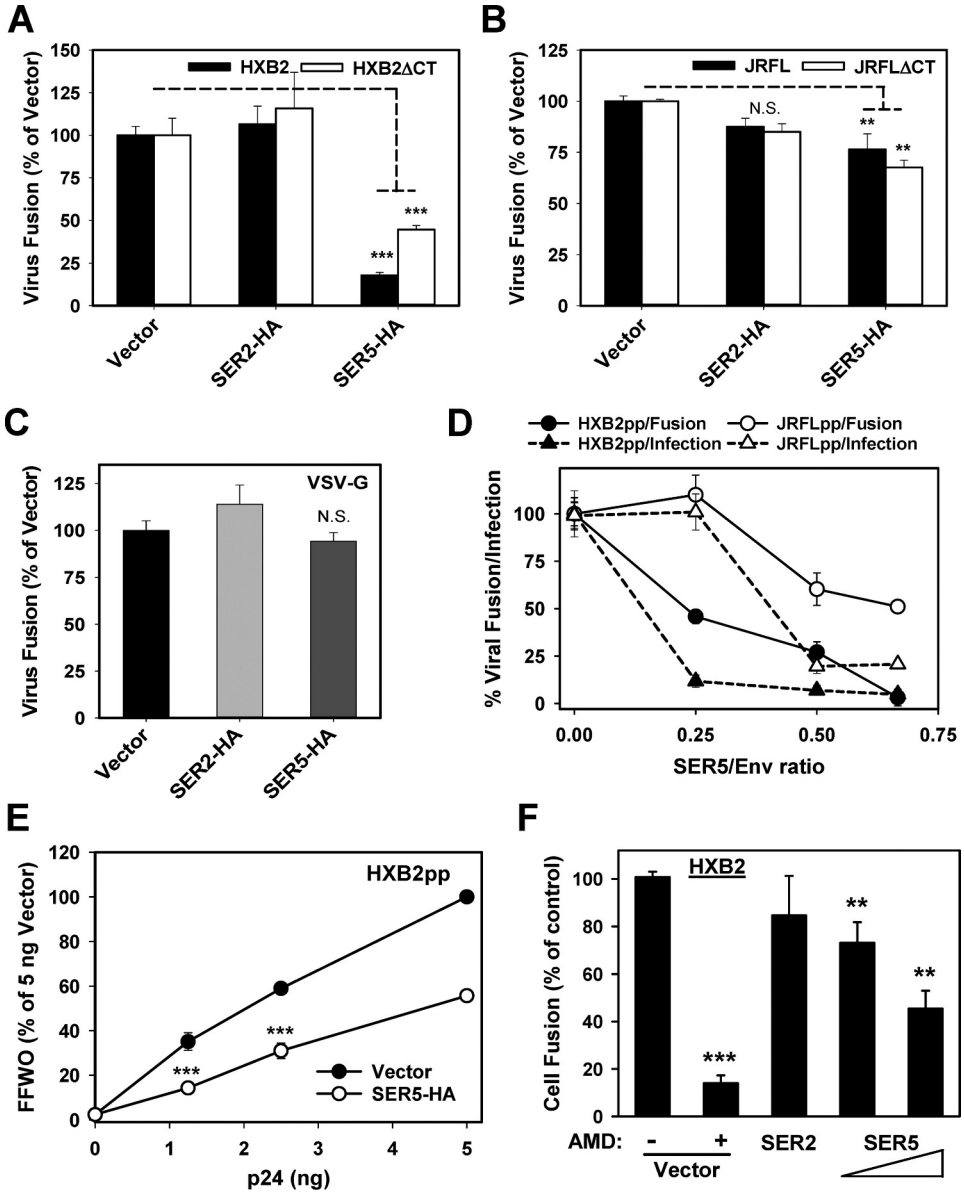

Figure 1. SER5 inhibits HIV-1 fusion. *A–C,* Nef-negative HIV-1 pseudoviruses bearing full-length or cytoplasmic tail-deleted (ΔCT) HXB2 Env, JRFL Env, or VSV-G, either lacking or containing SER5-HA, were allowed to enter TZM-bl cells, and the resulting fusion was measured by the BlaM assay. *N.S.*, not significant. *D,* comparison of virus fusion and infection in TZM-bl cells for HXB2pp and JRFLpp produced in cells transfected with increasing amounts of the SER5-HA plasmid and constant amount of the Env plasmid. *E,* effect of SER5 on FFWO mediated by HXB2pp. Increasing p24 quantities of HXB2pp produced in the presence or absence of SER5-HA were added to a mixed confluent monolayer of N4X4-DSP-1 and N4X4-DSP-2 cells by spinoculation. Fusion was allowed to proceed for 2 h at 37 °C. Data are mean and S.E. of two independent experiments in triplicate. *F,* inhibition of HXB2 Env-mediated cell-cell fusion by SER5. The N4X4-DSP-2 cells were overlaid with 293-DSP-1 cells transiently transfected with equal amounts of full-length HXB2 Env and SER2-GFP, SER5-GFP, or empty vector or 4:1 ratio of Env/SER5 (penultimate bar). The fusion efficiency was measured after 2 h by dual-split luciferase assay, as in *E*. Viruses lacking SER5 (*Vector*) were additionally treated with 100 μM AMD3100 as negative control. Data are mean and S.D. of two independent experiment in triplicates.

SER5 inhibits the formation of a small fusion pore between HIV-1 and a target cell and that this effect is Env-dependent. We demonstrate that HIV-1 fusion is inhibited through enhanced spontaneous inactivation of SER5-sensitive HIV-1 Env glycoproteins but not resistant Env. In addition, SER5 sensitizes HIV-1 to gp41-derived inhibitory peptides and neutralizing antibodies against cryptic functionally important gp41 domains. These effects are likely caused by SER5-mediated structural changes in HIV-1 gp41 and by slowing down its refolding that culminates in the formation of the final 6-helix bundle structure.

Results

SER5 inhibits HIV-cell fusion and Env-mediated cell-cell fusion

To assess the effect of SER5 on HIV-cell fusion, we compared the fusion activity of pseudoviruses that contained or lacked SER5 in their membrane or contained the inactive SER2 variant as a control. SER5, but not SER2, inhibited HIV-1 fusion, as measured by the BlaM assay (Fig. 1*A*). In agreement with the previous reports (10, 11), SER5 incorporation had a more pronounced effect on fusion of particles pseudotyped with HXB2 Env (HXB2pp) than those pseudotyped with JRFL Env

(JRFLpp), albeit JRFLpp fusion was significantly inhibited (Fig. 1, *A* and *B*). This inhibitory effect was not a result of gross SER5 overexpression in producer cells, because HXB2pp fusion could be partially or fully rescued by ectopic expression of HIV-1 Nef or MLV glycoGag in these cells (supplemental Fig. S1). The inhibitory effect of SER5 was not caused by reduced incorporation of HIV-1 Env or by interference with its proteolytic processing (supplemental Fig. S2*A*).

SER5 also inhibited fusion mediated by other HIV-1 clade B and clade A Env glycoproteins to a varied degree (supplemental Fig. S3, *A*–*C*), and the inhibitory effect appeared to be largely independent of the target cells (supplemental Fig. S3, *D* and *E*). By contrast, and as reported previously (10, 11), VSVpp fusion was relatively resistant to SER5 (Fig. 1*C*). However, in agreement with Ref. 11, VSVpp incorporated less SERINC proteins as compared with HIV-1 Env pseudotypes (supplemental Fig. S2*B*). We also found that both SERINCs were somewhat less abundant in JRFLpp as compared with HXB2pp in two independent preparations (supplemental Fig. S2*A* and data not shown).

Parallel viral fusion experiments revealed that the cytoplasmic tail (CT) of Env did not consistently modulate the inhibitory effect of SER5. Although SER5 was somewhat less active against fusion of particles pseudotyped with the tail-deleted HXB2 Env (ΔCT) than against full-length Env (Fig. 1*A*), this effect was reversed for JRFL Env (Fig. 1*B*). Thus, the modest differences in SER5 sensitivity of the full-length and tail-deleted Env could be due to the efficiency of their incorporation into virions and/or proteolytic processing.

SER5 suppressed HIV-1 fusion in a dose-dependent manner; progressive reduction in the fusion signal was observed upon increasing the ratio of SER5- to Env-expressing plasmid used to transfect the producer cells (Fig. 1*D*). Western blotting confirmed that viruses harvested from cells transfected with increased amounts of SER5 or SER2 plasmids incorporated proportionally more SERINC proteins (supplemental Fig. S2*C*). Interestingly, for a given SER5/Env ratio, SER5 more potently suppressed single cycle HIV-1 infection compared with fusion (Fig. 1*D*). A stronger inhibition of infection *versus* fusion by SER5 has been reported in the recent studies (10, 11) and interpreted as interference with the fusion pore enlargement and, thereby, with the release of HIV-1 capsid.

We next tested whether pseudoviruses carrying SER5 were impaired in their ability to mediate syncytia upon fusing with the plasma membranes of two adjacent cells, a phenomenon referred to as "fusion-from-without" (FFWO) (19). We have previously shown that FFWO is very inefficient and highly dependent on actin dynamics, in contrast to virus-cell fusion (20). Virus-mediated cell-cell fusion was assessed using a dual-split luciferase assay that produces a robust luciferase signal upon fusion between two target cell lines expressing the complementary split GFP-luciferase protein fragments (21). SER5-containing viruses less efficiently induced FFWO compared with control viruses (Fig. 1*E*). For the same ratio of SER5/Env plasmids used to obtain HXB2 pseudoviruses, virus-cell fusion and FFWO were inhibited to a comparable extent (Fig. 1, *D* and *E*). Considering that HIV-cell fusion appears to occur in endocytic compartments (22–24), whereas FFWO results from virus fusion with the plasma membrane, the above findings imply that SER5 attenuates the virus' ability to fuse irrespective of the entry site.

To determine whether SER5 antagonizes the HIV-1 Env-mediated membrane fusion in the absence of other viral proteins, we measured fusion between CD4/coreceptor-expressing cells and cells expressing Env and SER5 (or SER2 as control). SER5 but not SER2 inhibited HXB2 Env-mediated cell-cell fusion (Fig. 1*F*) without significantly altering the expression of Env glycoprotein on the cell surface (supplemental Fig. S3, *F* and *G*). Comparable effects of SER5 on HXB2 Env-mediated virus-cell and cell-cell fusion (Fig. 1, *A*, *D* and *F*) argue against the involvement of other viral proteins in the SER5 restriction phenotype. To conclude, SER5 interferes with membrane fusion mediated by sensitive HIV-1 Env, while having a modest or no effect on resistant viral glycoprotein.

SER5 incorporation does not trap HIV-1 at a dead-end hemifusion state or target virus to lysosomal degradation

A preponderance of evidence implies that viral and cellular protein-mediated fusion progresses through a hemifusion intermediate defined as lipid mixing without content transfer, which requires opening of a fusion pore (25). To determine whether SER5 blocks the transition from hemifusion to fusion, we treated cells at 30 min post-infection with chlorpromazine (CPZ) to mediate conversion of hemifusion to full fusion (26, 27). This treatment did not affect the extent of fusion of control (or SER2+) HXB2pp or rescue fusion of SER5+ pseudoviruses (Fig. 2*A*). In contrast, VSVpp fusion was significantly enhanced by CPZ, irrespective of the presence of SER5 (Fig. 2*B*), suggesting the formation of a considerable fraction of dead-end hemifusion structures upon entry of this pseudovirus. Under these experimental conditions, exposure to CPZ did not adversely affect cell viability (Fig. 2*C*). We concluded that SER5 does not stall the transition from hemifusion to fusion and acts through an alternative mechanism.

Because HIV-1 appears to infect TZM-bl cells by an endocytic route (23, 24), we asked whether diminished viral fusion observed in our experiments resulted from an accelerated degradation of SER5+ virions in late endosomes/lysosomes as compared with control viruses. The extent of lysosomal degradation of fusion-competent SER5+ viruses was evaluated by inoculating cells with pseudoviruses in the presence of BafA1 to block endosomal acidification and interfere with virus degradation. BafA1 only marginally (albeit significantly) increased the fusion efficiency of SER5+ HXB2pp compared with untreated control or to viruses lacking SER5 (Fig. 2*D*). This result argues against excessive virus degradation as the basis for the markedly reduced fusion efficiency of SER5+ particles.

SER5 but not SER2 inhibits the formation of small fusion pores

To determine which step of HIV-1 fusion downstream of hemifusion is antagonized by SER5, we imaged single virus fusion with living cells. HXB2pp were co-labeled with YFP-Vpr and the viral content marker Gag-iCherry containing an "internal" mCherry tag (28). Fusion of HXB2pp containing or lacking SER5-HA or SER2-HA culminates in the release of mCherry through fusion pores larger than 4 nm in diameter (Fig. 3, *A* and

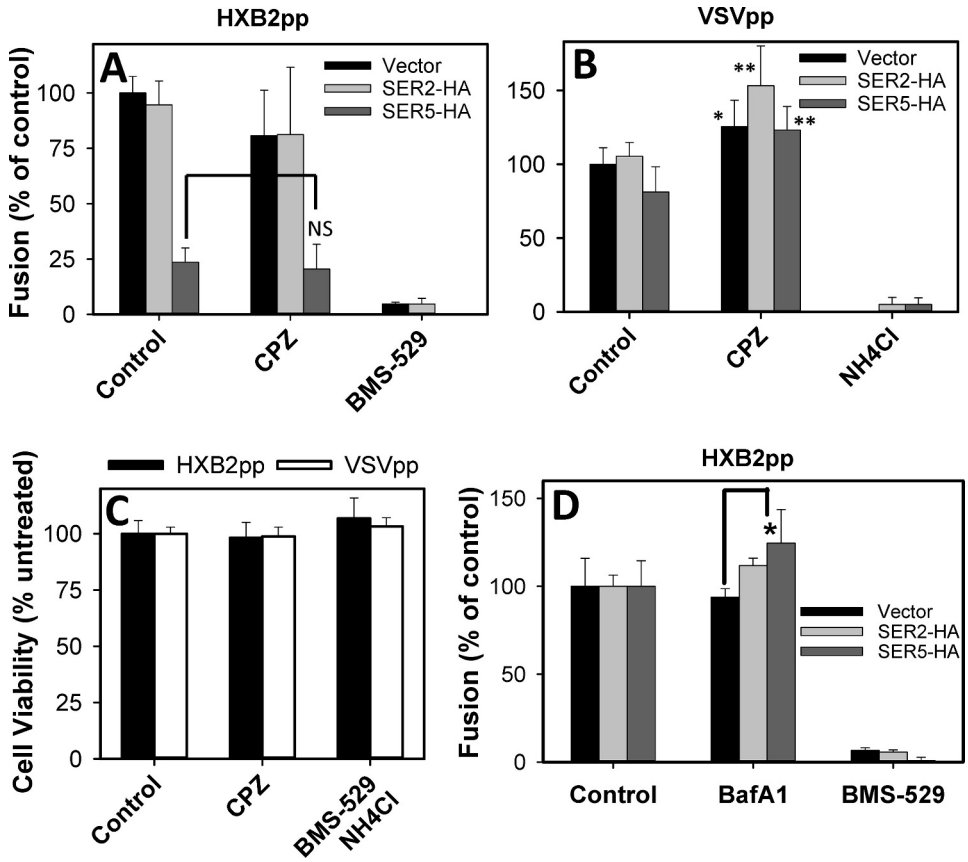

Figure 2. SER5 does not considerably promote lysosomal degradation of HIV-1 or stall fusion at a hemifusion stage. *A,* fusion of HXB2pp containing or lacking SERINCs with TZM-bl cells was synchronized by pre-binding the virus in the cold and shifting to 37 °C. After 30 min at 37 °C, cells were treated with 0.5 mM CPZ for 30 s and washed, and incubation was continued for 60 min. BMS-529 (10 μM) was added to control wells to block HXB2pp fusion. *B,* CPZ treatment promotes VSVpp fusion independent of the presence of SERINCs. The VSVpp fusion protocol and the CPZ treatment step were as in *A*. Negative control included NH_4Cl (70 mM). Data are mean and S.E. of two independent experiments in triplicate. *C,* cell viability for the experiments in *A* and *B*. *D,* SER5-HA viruses are marginally more degraded compared with control viruses. HXB2pp containing or lacking SERINCs were pre-bound to TZM-bl cells in the cold and incubated at 37 °C for 90 min in the presence or absence of 50 nM BafA1 or 10 μM of the HIV-1 fusion inhibitor BMS-529. Virus-cell fusion was measured by the BlaM assay. Data are mean and S.E. of two independent experiments in triplicate.

B) (28). As expected, SER2-HA-containing particles and control virions fused equally well, whereas fusion of SER5-HA particles was markedly inhibited (Fig. 3*C*). The extent of SER5 virus fusion (<0.2% of double-labeled particles) was indistinguishable from fusion of SER2-HA particles in the presence of the CXCR4 antagonist AMD3100. For the HXB2pp preparations used in the fusion experiments, incorporation of SER2 into virions was even more efficient than SER5 incorporation (Fig. 3*D*, *inset*), but only SER5 strongly inhibited infectivity (Fig. 3*D*).

The supplemental Fig. S2 shows that SER5 incorporation does not interfere with Env incorporation. We also verified the lack of SER5 effect on Env incorporation into fluorescently labeled pseudoviruses used for imaging. Immunostaining for Env (2G12 antibody) and for SER5 (anti-HA) revealed that the distribution of Env signal was not affected by the amount of virus-incorporated SER5 (Fig. 3, *E* and *F*). We thus concluded that SER5 specifically inhibits the formation of small fusion pores between HXB2pp and the target cell.

HIV-1 env does not stably interact with SER5 or form large aggregates in the plasma membrane

We next asked whether SER5 antagonizes the Env function by directly binding to the fusion protein. Lysates of mock-transfected 293T cells or cells transfected co-expressing SER5-HA or SER2-HA and HXB2 Env were immunoprecipitated using anti-HA tag antibody or HIV immune serum. This pulldown assay did not show any evidence for Env-SER5 interactions (supplemental Fig. S4). It is possible, however, that weak and/or transient interactions between SER5 and Env escape the detection by this assay.

A possible mechanism by which SER5 can antagonize HIV-1 fusion without directly interacting with Env is through modification of the viral membrane. For instance, the formation of large SER5 oligomers can inhibit fusion by restricting lipid diffusion and/or stiffening the viral membrane. Because protein oligomerization should be manifested in slower mobility in membranes, the lateral diffusion of SER5-GFP and GFP-tagged CCR5 (control multi-transmembrane protein) was measured by fluorescence recovery after photobleaching (FRAP). We found that neither the calculated diffusion coefficient nor the immobile fraction of SER5-GFP was significantly different from those of CCR5-GFP (Fig. 4). Because SER5 diffuses freely in the plasma membrane, the reduction in membrane fluidity or the formation of large SER5-enriched domains are unlikely to underlie its ability to inhibit viral fusion. However, we cannot rule out the possibility that

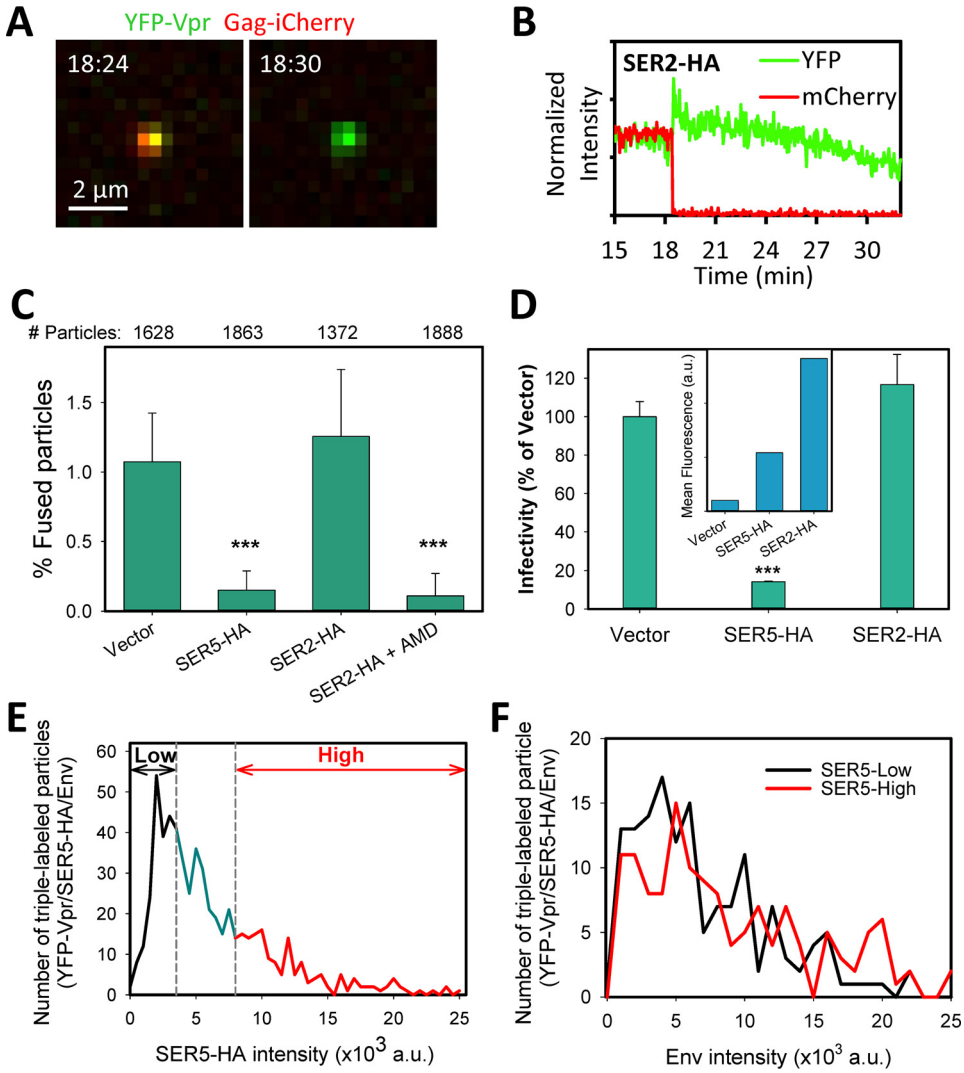

Figure 3. SER5 restricts fusion pore formation between single HXB2pp and target cell. HXB2pp co-labeled with YFP-Vpr and Gag-iCherry were produced in cells transfected with SER5-HA, SER2-HA, or an empty vector. Virions were pre-bound to CD4/CXCR4-expressing CV1 cells in the cold, and their fusion was initiated by shifting to 37 °C. *A* and *B,* images and single particle tracking results for fusion of SER2-HA containing HXB2pp showing the release of the mCherry marker. *C,* analysis of the effect of SER5 and SER2 on single HXB2pp fusion in the absence or in the presence of 10 μM AMD3100. Data are means and S.D. from 4 to 5 independent experiments. The numbers of double-labeled particles analyzed for each condition are shown above the graph. *D,* infectivity of the viral preparations analyzed in *C* in TZM-bl cells. *Inset,* percent fluorescent virions after immunostaining for HA tag to control for SER2/SER5 incorporation. *E,* SER5-HA fluorescence intensity distribution from imaging single pseudoviruses immunostained with anti-HA and 2G12 antibodies. Arbitrary classification of particles based on their low and high SER5 content is shown (*black* and *red lines*). *F,* Env content (2G12 staining intensity) distribution for low *versus* high SER5 particles (*black* and *red lines*, respectively).

SER5 may be enriched in the viral membrane and thus be more prone to aggregate.

SER5 enhances HIV-1 sensitivity to neutralizing antibodies and inhibitory peptides that recognize conserved gp41 domains transiently exposed during viral fusion

To elucidate the mechanism by which SER5 inhibits HIV-1 fusion, we probed the effect of this protein on exposure of cryptic Env domains during viral fusion. The extent of exposure of the functionally relevant Env domains in control and SER5+ viruses was examined by comparing the sensitivity to neutralizing antibodies against the gp41 membrane-proximal extracellular region (MPER) and the HR1 domain that are transiently exposed during HIV-1 fusion (29–32). Incorporation of SER5 sensitized the HIV-1 fusion to 4E10, a broadly neutralizing antibody against the gp41 MPER (Fig. 5*A*). The Fab fragment of 8k8 antibody against the gp41 HR1 domain (33) also more potently inhibited fusion of SER5+ than control viruses (Fig. 5*B*), although the effect was not as strong as for 4E10 antibody. SER2, which does not significantly affect HXB2 fusion (Fig. 1), did not impact the virus' sensitivity to 4E10 and 8k8 (Fig. 5, *A–F*). SER5 also enhanced the neutralizing activity of 4E10 against JRFLpp and BaLpp (Fig. 5, *E* and *F*), in excellent agreement with the previously reported potent neutralization of Nef-deficient HIV-1 and of SER5-containing virions by this antibody (16, 34).

By contrast, SER5 did not affect the inhibitory activity of the broadly reactive 2G12 antibody that recognizes a conformation-independent glycan cluster on the gp120 (Fig. 5, *C* and *D*) (35, 36). Furthermore, it did not noticeably alter the potency of several other anti-gp120 antibodies, including the broadly neutralizing PG16 antibody against a quaternary glycan-containing

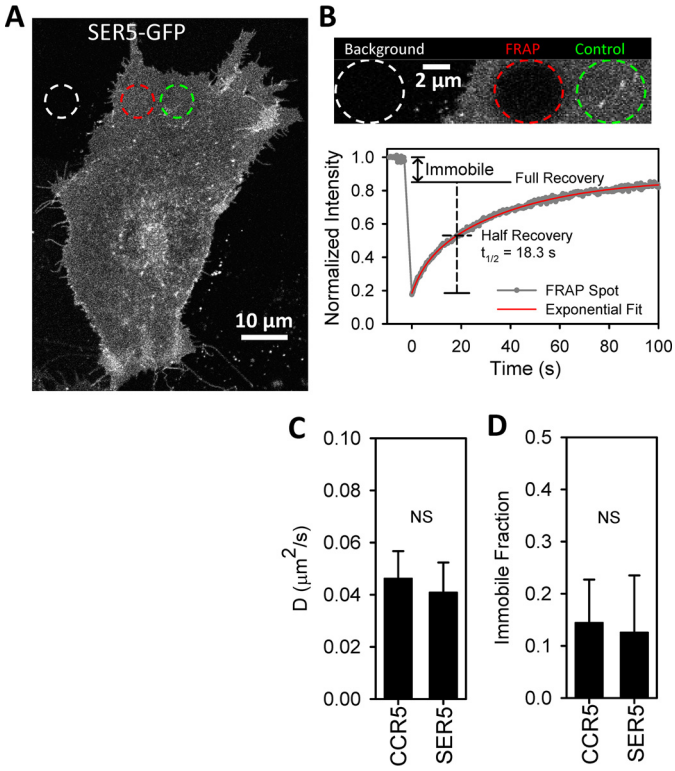

Figure 4. SER5 and CCR5 display similar long range mobility in the plasma membrane. SER5-GFP or CCR5-GFP was transiently expressed in CV-1 cells. *A,* small circular regions within the basal plasma membrane of a CV-1 cell transfected with SER5-GFP were photobleached, and recovery of fluorescence over time was measured. *B, top,* small section of the plasma membrane scanned during FRAP acquisition shows circular areas used for measuring background, fluorescence recovery, and control intensity (*circled white, red,* and *green*, respectively) immediately after bleaching. *B, bottom,* corrected trace of sum intensity in the FRAP region was fit to an exponential rise function to calculate the half-time of intensity recovery ($t_{1/2}$) and immobile fraction. *C* and *D,* comparison of the diffusion coefficient (*C*) and immobile fraction (*D*) of CCR5-GFP and SER5-GFP expressed in the plasma membrane. Data are mean and S.D. of two experiments (>10 measurements for each condition).

epitope on the native Env trimer, as well as the antibodies m36 and 17b to CD4-induced gp120 epitopes (supplemental Fig. S5). These results indicate that SER5 does not modulate antigenic properties of gp120 or enhance the exposure of cryptic gp120 epitopes during fusion.

Enhanced HIV-1 neutralization by antibodies recognizing cryptic gp41 epitopes can result from exposure of these epitopes on unliganded Env or from slower gp41 refolding that prolongs the lifetime of the gp41 pre-hairpin intermediate. To determine whether SER5 alters the gp41 structure prior to Env-CD4 engagement, 4E10 binding to single coverslip-adhered pseudoviruses was measured by indirect immunofluorescence. The background-corrected fluorescence intensities were measured for each mCherry-Vpr-labeled particle lacking or containing SER5-GFP or SER2-GFP. Specific infectivity for the analyzed preparations was determined to ensure proper restriction of the Env function by SER5 (Fig. 5*G*). To account for variations in Env incorporation between different preparations and for possible gp120 shedding, median 4E10 intensity values were normalized to values obtained in parallel experiments using a control 2G12 antibody. Incorporation of SER5 into HXB2pp did not significantly increase the 4E10/2G12 binding ratio (Fig. 5*H* and supplemental Fig. S6). By contrast, the relative 4E10 binding was significantly enhanced for SER5+ JRFLpp compared with vector or SER2 viruses (Fig. 5*H* and supplemental Fig. S6). In control experiments, treatment of either HXB2pp or JRFLpp with soluble CD4 (sCD4) enhanced the relative 2G12 binding, in agreement with a previous report (37). Our results suggest that the MPER is more accessible on SER5+ JRFLpp, in line with a more efficient 4E10-mediated neutralization of this virus as compared with control JRFLpp (Fig. 5*E*). The lack of SER5 effect on the 4E10 binding to HXB2pp could reflect the natural tendency of this Env to expose MPER or result from possible functional inactivation of Env that sequesters this region (see under "Discussion") (30).

To assess whether the increased potency of anti-gp41 antibodies could be due to a prolonged exposure of the HR1 domain during fusion, we assessed the virus' sensitivity to the gp41 HR2-derived peptides C34 and T-20 (referred to as C-peptides). These peptides bind to the HR1 domain transiently exposed on pre-hairpin intermediates (similar to the 8k8 antibody (33)) and block the 6-helix bundle formation (38). Fusion of SER5-containing HXB2pp and JRFLpp was inhibited by 2–4-fold lower doses of C-peptides than fusion of control or SER2+ viruses (Fig. 6, *A–D*). The higher sensitivity to C-peptides is consistent with the prolonged exposure of gp41 pre-hairpins in the course of viral fusion (39–44). Collectively, the above results suggest that SER5 may cause structural changes in the native HIV-1 gp41 trimer and potentially slow down the gp41 refolding into the final 6-helix bundle structure.

SER5 specifically promotes inactivation of sensitive HIV-1 Env

We next examined the effect of SER5 on the functional stability of Env. HXB2pp preincubation at 37 °C for 4 h promoted spontaneous loss of the fusion activity and infectivity, and this loss was markedly accelerated in the presence of SER5 (Fig. 7, *A* and *B*). In contrast, a 37 °C preincubation only modestly diminished the ability of JRFLpp and VSVpp to fuse or infect target cells, irrespective of the presence of SER5. SER5 incorporation also accelerated inactivation of other HIV-1 strains, albeit to a lesser extent than HXB2 Env (Fig. 7, *C* and *D*). As expected, SER2 did not significantly modulate the loss of HXB2pp fusion activity. Unlike the fusion activity, the infectivity of HXB2pp and JRFLpp containing SER2 was modestly reduced compared with control viruses following a preincubation at 37 °C (Fig. 7, *A* and *B*).

The accelerated functional inactivation of HXB2 Env, but not JRFL Env or VSV-G, in SER5-containing virions phenocopies the differential sensitivity of these fusion proteins to SER5 (Figs. 1, *A–C,* and 7) (10, 11). To conclude, the above results establish an important link between the inherent stability of Env trimers and sensitivity to SER5, because the resistant fusion proteins appear to be less prone to spontaneous inactivation.

Discussion

Our results demonstrate that SER5 inhibits HIV-cell fusion and Env-mediated cell-cell fusion at the stage of small pore formation and link this effect to the following: 1) promotion of spontaneous inactivation of sensitive (HXB2) but not of resistant (JRFL or VSV) viral fusion proteins; 2) alteration of the gp41

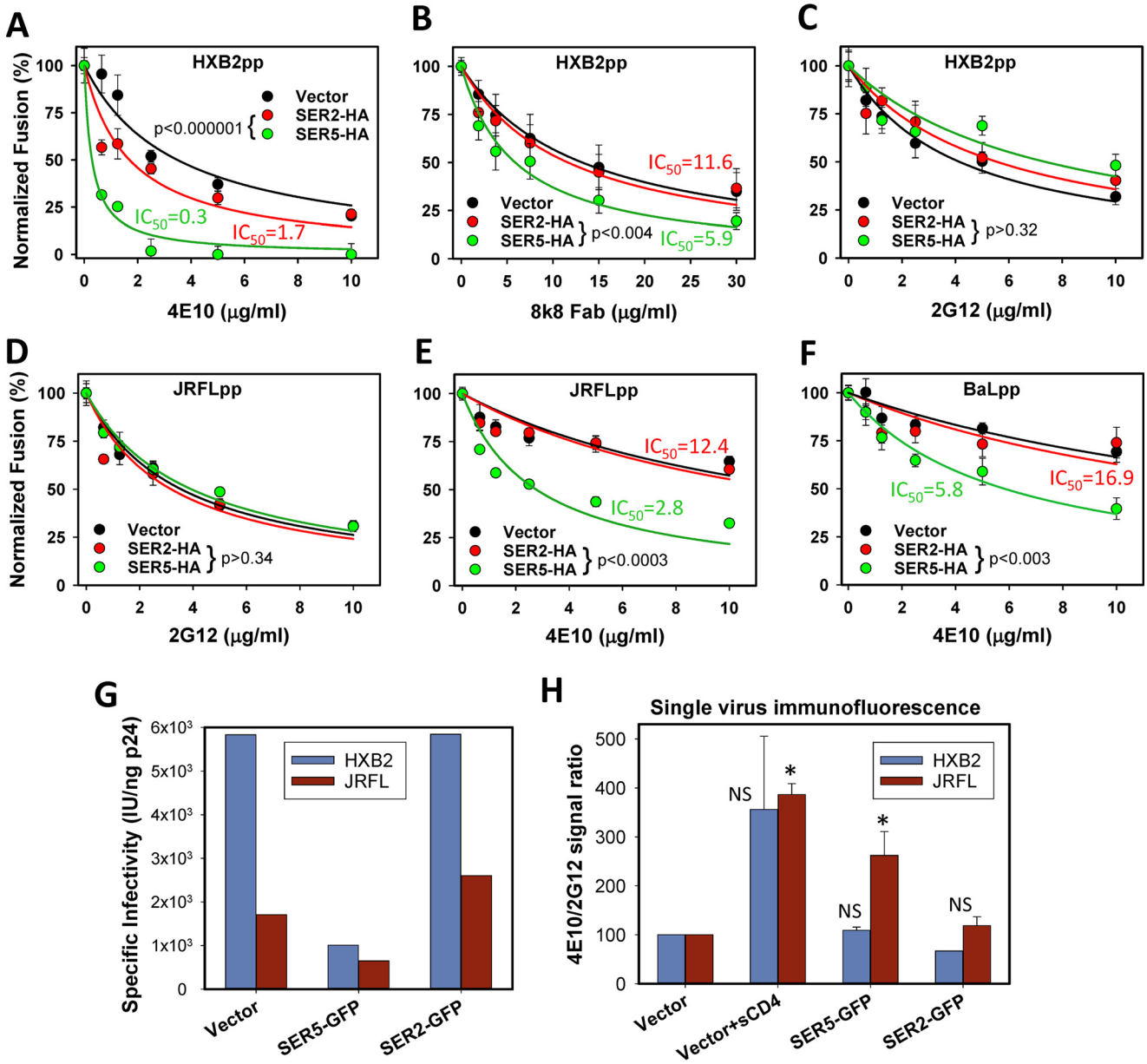

Figure 5. SER5 potentiates the neutralizing activity of antibodies and peptides against cryptic gp41 epitopes exposed during fusion. *A–F,* HIV-1 particles pseudotyped with HXB2, JRFL, or BaL26 Env, lacking or containing SER5-HA or SER2-HA, were used to inoculate TZM-bl cells, and the resulting fusion was measured by the BlaM assay. Indicated concentrations of neutralizing antibodies were added after virus pre-binding in the cold, immediately before raising the temperature. Data are means of two independent experiments performed in triplicate. The IC_{50} values obtained by curve-fitting and statistical significance of the effects of SER5 on HIV-1 sensitivity to neutralization (sum of squares reduction test) are shown on the plots. *G* and *H,* specific infectivity (*G*) and 4E10/2G12 median single-particle staining intensity ratio (*H*) for HXB2pp and JRFLpp. Data are means and S.D. from two independent experiments. The sCD4-induced increase in 4E10 binding was statistically significant for JRFLpp but not HXB2 particles due to a large variance between the immunofluorescence experiments. See also supplemental Fig. S6.

structure; and 3) delayed gp41 refolding into the final trimer-of-hairpins structure. Importantly, these SER5 effects are specific, as the inactive SER2 variant does not accelerate the loss of the HIV-1 fusion competence, alter the virus sensitivity to fusion inhibitors, or increase the accessibility of the gp41 MPER to neutralizing antibodies.

Selective inactivation of sensitive HIV-1 Env by SER5 phenocopies the known restriction specificity (10, 11, 18), suggesting a connection between the SER5 restriction efficiency and inherent stability of native Env trimers (45–47). The differences in the predicted stoichiometry of oligomeric Env complexes required for productive fusion/infection (48) can exacerbate the SER5 effect on the sensitive HIV-1 strains. A greater number of SER5-sensitive NL4-3 and SF162 Env per virion is required to mediate productive entry compared with the less sensitive JRFL Env (4–7 *versus* 2 Env, respectively (48)). Thus, partial inactivation of JRFL Env should be less consequential for fusion than inactivation of Envs on NL4-3 or HXB2 virions that must stochastically assemble larger Env complexes to promote fusion.

Although we found that SER5 inhibits small pore formation, excessive functional inactivation of Env is also in line with interference with pore enlargement required for the viral capsid release, as proposed based upon a more potent inhibition of

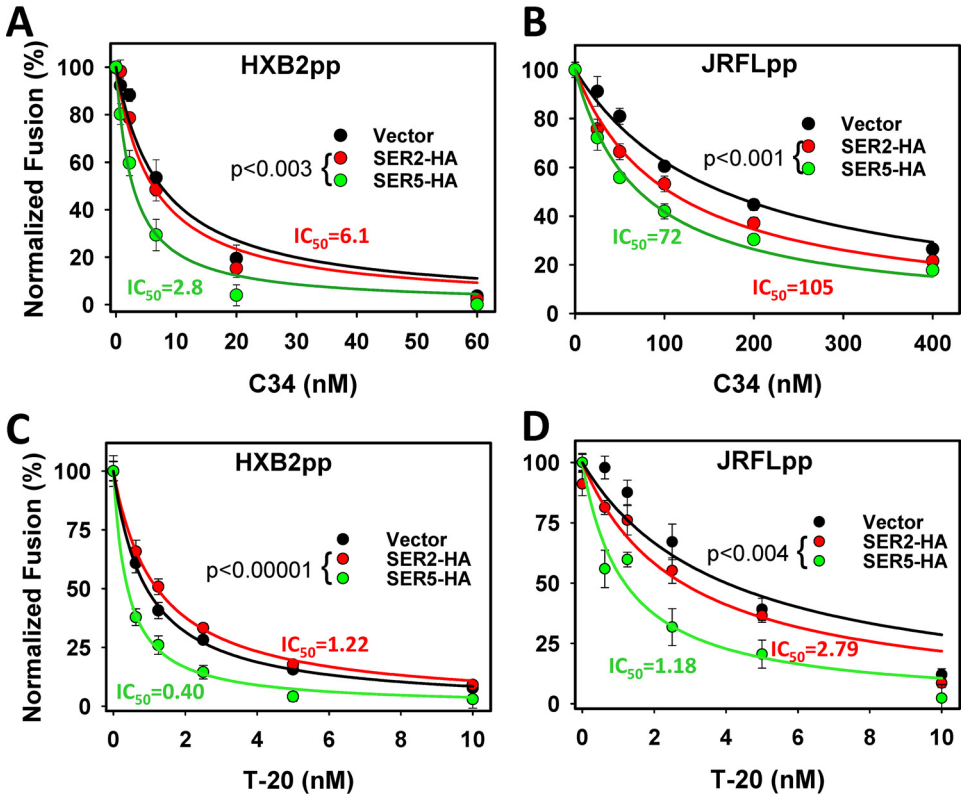

Figure 6. Enhanced sensitivity of HXB2 and JRFL pseudoviruses to inhibition by gp41-derived peptides. *A* and *B*, dose-dependent inhibition of control and SER2- or SER5-containing HXB2pp and JRFLpp by C34. *C* and *D*, effect of SER5 on sensitivity of HXB2pp and JRFLpp to T-20 peptide. Virus fusion with TZM-bl cells was measured by the BlaM assay. Data are means of two independent experiments performed in triplicate. The IC_{50} values obtained by curve-fitting and statistical significance of the SER5 effects on the HIV-1 sensitivity to inhibitory peptides, as determined by the sum of squares reduction test, are shown on the plots.

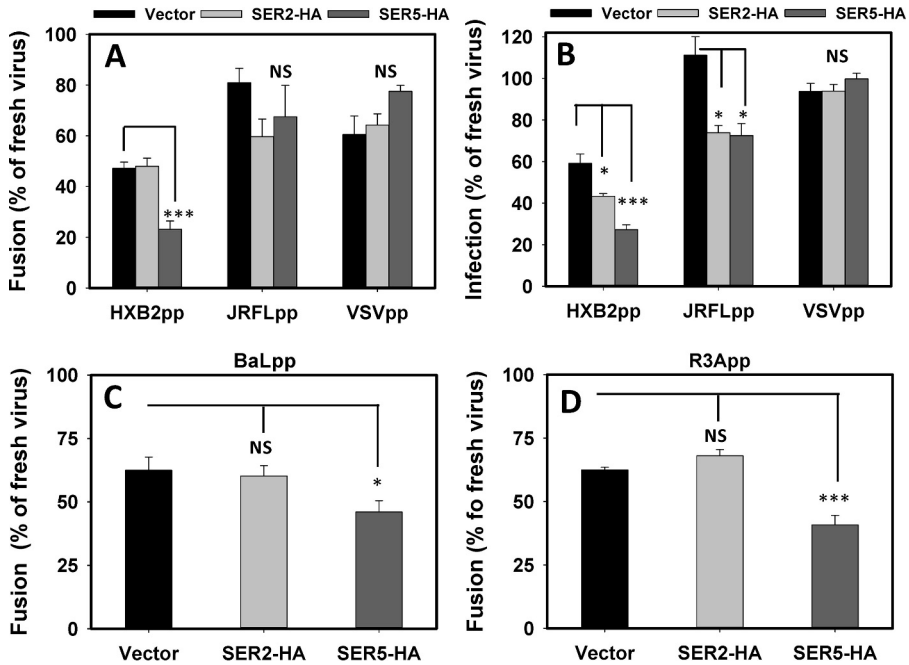

Figure 7. SER5 selectively promotes functional inactivation of HXB2 Env. *A*, Nef-negative HIV-1 particles pseudotyped with HXB2 Env, JRFL Env, or VSV-G, containing or lacking SER5-HA or SER2-HA, were preincubated in growth medium containing 10 mM HEPES (pH 7.3) for 4 h at 37 °C or used immediately after thawing the samples (fresh). Viruses were bound to TZM-bl cells in the cold by spinoculation, and cells were washed and incubated at 37 °C for 90 min. The fusion efficiency measured by the BlaM assay was normalized to the respective freshly initiated virus. *B*, pseudovirus infectivity was measured using conditions described in *A*. *C* and *D*, SER5 promotes spontaneous inactivation of pseudoviruses bearing BaL and R3A Env, as measured by a virus-cell fusion assay after a 4-h preincubation at 37 °C, as above. Data are mean and S.E. of two independent experiments in triplicates.

HIV-1 infection than fusion by this protein (10, 11). Fewer functional Env glycoproteins on SER5-containing viruses are less likely to drive pore dilation, which is a highly energetically unfavorable step of membrane fusion (49, 50). The development of direct viral pore enlargement/core release assays is needed to determine whether SER5 incorporation inhibits HIV-1 core release.

We found that SER5 but not SER2 incorporation facilitates the binding of anti-MPER 4E10 antibody to the native JRFL Env, in agreement with the recent studies (16, 34) and consistent with the enhanced exposure of the gp41 MPER. Strangely, Beitari *et al.* (16) did not detect SER5 effects on HIV-1 neutralization by other anti-MPER antibodies, such as 2F5 and 10E8. In this context, it is worth noting that the 4E10 binding to virions is lipid-dependent, with considerable affinity to negatively charged lipids, including PS, whereas the binding of 2F5 and 10E8 is less affected by this lipid (51). Thus, the enhanced 4E10 binding to SER5+ JRFLpp may be caused by the increased PS content and not just by the MPER exposure. Whereas this model could reconcile discrepant findings regarding the effect of SER5 on binding of anti-MPER antibodies (16), the lack of effect on binding to HXB2 pseudoviruses (Fig. 5*H*) and the apparently similar levels of PS in control and SER5+ particles (15) are inconsistent with this possibility. We surmised that the similar extents of 4E10 binding to control and SER5+ HXB2pp may be caused by the excessive HXB2 gp41 MPER exposure in the absence of the restriction factor and/or from the functional inactivation of this Env on SER5+ virions, which may sequester the MPER domains (30).

Finally, SER5 appears to slow down gp41 refolding triggered upon gp120-CD4/coreceptor engagement, as evidenced by the increased sensitivity to C34 and T-20 and to neutralizing antibodies against the gp41 HR1 domain. Although a recent study did not observe an SER5 effect on the anti-HIV-1 potency of the T-20 peptide (16), the discrepancy could be due to the use of a V3 loop Env chimera in the latter study and/or to the differences in the virus-cell fusion protocols. Collectively, our results are consistent with both SER5-mediated structural changes, at least within the gp41 MPER domain, and with slowing down the gp41 refolding.

Although direct SER5-Env interaction could not be detected by a co-immunoprecipitation assay, we surmise that SER5 may partition into the same lipid domains in the viral membrane as Env and act as a physical barrier for functional Env clustering. The unusually high cysteine content of SER5 supports its affinity for lipid rafts into which Env glycoproteins tend to partition. The fact that SER2 lacks 11 of the Cys residues present in SER5 supports the possibility of selective SER5 interference with functional Env oligomerization and/or modulation of lipid composition of the viral membrane. Further studies are needed to determine how SER5 destabilizes the native Env glycoprotein and inhibits the viral fusion pore formation and possibly pore dilation. Toward this goal, it is essential to delineate the SER5 effect on the viral lipid composition and the propensity of Env trimers to form functional clusters in the viral membrane.

Experimental procedures

Cell lines, reagents, and plasmids

HEK293T/17 and CV-1 cells were obtained from ATCC (Manassas, VA). TZM-bl cells were from the AIDS Research and Reference Reagent Program (National Institutes of Health) (donated by Drs. J. C. Kappes and X. Wu (52)). The CV-1/CD4/CXCR4 (CF3 clone) cells were a gift from Dr. David Kabat (Oregon State University), and 293T-DSP-1 and NP2/CD4/CXCR4/DSP-2 cell lines were a gift from Dr. Aikichi Iwamoto (University of Tokyo) (20, 22). NP2/CD4/CXCR4/DSP-2 cells were grown in minimum Eagle's medium supplemented with 10% FBS, 100 units/ml penicillin/streptomycin, and 4 μg/ml blasticidin (Bioworld, Atlanta, GA). All the other cell lines were cultured in DMEM supplemented with 10% fetal bovine serum and 100 units/ml penicillin/streptomycin (Gemini Bio-Products, Sacramento, CA). The growth medium for HEK293T/17 cells was supplemented with 0.5 mg/ml G418 (Cellgro, Mediatech, Manassas, VA).

EnduRen™ and Bright-Glo luciferase were from Promega (Madison, WI). Heat-inactivated fetal bovine serum (FBS), poly-L-lysine, calf skin collagen, and AMD3100 were from Sigma. Live Cell Imaging Buffer and FluoroBrite™ DMEM were from Life Technologies, Inc. The BMS-626529 was purchased was from AURUM Pharmatech LLC (Franklin Park, NJ). The gp41-derived C34 peptide was a gift from Dr. L. Wang (University of Maryland, Baltimore). The following reagents were obtained from the AIDS Reagent Program, Division of AIDS, NIAID, National Institutes of Health: pcDNA3.1 vector expressing HIV-1 BaL envelope glycoprotein (clone BaL.01, Dr. J. Mascola, National Institutes of Health) (53); pSVIII-92UG037.8 HIV-1 envelope glycoprotein (Dr. Feng Gao and Dr. Beatrice Hahn, and the DAIDS, NIAID, National Institutes of Health) (54); pcRev (Dr. Bryan R. Cullen) (55); pMM310-BlaM-Vpr (Dr. Michael Miller, Merck Research Laboratories) (6); HIV immunoglobulin (HIV Ig) (Dr. Luiz Barbosa, NABI, NHLBI, National Institutes of Health); HIV monoclonal antibodies (mAbs) PG16 (from IAVI, La Jolla, CA) (56); 17b (Dr. J. Robinson, Tulane University Medical Center) (57); 4E10 and 2G12 (Dr. Hermann Katinger, POLYMUN Scientific GMBH) (58, 59); T-20 (*N*-acetylated derivative from Roche Applied Science); and human recombinant soluble CD4 protein (Progenics). The antibody m36 was a gift from Dr. D. Dimitrov (NCI, National Institutes of Health, Frederick, MD); the 8K8 mAb was provided by Dr. M. Zwick (Scripps Research Institute, CA). The pCAGGS plasmids encoding HXB2, HXB2 140T, JRFL, JRFL 140T, and E168K/N189A envelope glycoproteins were provided by Dr. J. Binley (Torrey Pines Institute, CA). pHPG-R3A HIV-1 envelope glycoprotein was a gift from Dr. J. Hoxie (University of Pennsylvania). The pMDG-VSV-G plasmid expressing VSV-G was a gift from J. Young (Roche Applied Science, Mannheim, Germany). The HIV-1-based packaging vectors pR9ΔEnv and pR9ΔEnvΔNef were from Dr. Chris Aiken (Vanderbilt University). mCherry-Vpr, psPAX2-Gag-imCherry, PBJ5, PBJ5-SER5-HA, PBJ5-Nef LAI, PBJ5-glycoGag, CMV-SER2-GFP, CMV-SER5-GFP, and PBJ6-SER2-HA expression vectors have been described previously (10, 60, 61).

To obtain PBJ5-SER2-HA plasmid, the PBJ6-SER2-HA was digested with NotI and EcoRI restriction enzymes, and the fragment SER2-HA was purified on 1% agarose gel and ligated with PBJ5 digested and purified in similar manner. Construction of PBJ5-SER2-GFP and PBJ5-SER5-GFP was done as follows. The SER2-GFP gene fragment was amplified using *Taq*DNA polymerase high fidelity (Invitrogen), CMV-SER2-GFP plasmid as a template, and the forward and reverse primers 5′-GCGCTCGAGCGGCCGCCATGGACGGGAGGATGATGAG-3′ and 5′-GCTGCGGCCGCTTACTTGTACAGCTCGTCCATGCCGA-3′, respectively. The amplified fragment was inserted into pCR2-Topo vector using a TOPO cloning kit (Invitrogen). The SER2-GFP gene was digested with XhoI and NotI restriction enzyme sites (corresponding to the italicized regions in primers), purified, and ligated into PBJ5 digested and purified in an identical manner. The SER5-GFP was amplified using CMV-SER5-GFP plasmid as a template, and the forward 5′-GCGCTCGAGCGGCCGCCATGTCAGCTCAGTGCTGTGC-3′ and the same reverse primer as for SER2-GFP. The amplified fragments were purified and cloned into pCR2-Topo vector followed by restriction digestion with XhoI and NotI restriction enzymes and cloned into PBJ5 digested with the same restriction enzymes.

Pseudovirus production and characterization

HIV-1 pseudoviruses used in the BlaM assay and single virus experiments were produced by transfection of HEK293T/17 cells, as described previously (23, 28). Cells were transfected with the following amounts of plasmids per 100-mm dish: 3 μg of Env, 4 μg of pR9ΔEnv or pR9ΔEnvΔNef, 1.5 μg of pBJ5 or pBJ5-SER2-HA or pBJ5-SER5-HA (unless indicated otherwise), 2 μg of BlaM-Vpr, and 0.5 μg pcRev. To examine the effects of Nef or glycoGag, cells were transfected as above, except 2 μg of pBJ5-Nef LAI or pBJ5-glycoGag was added to the mix. To produce virus for imaging assays, HEK293T/17 cells on a 60-mm dish were transfected with 0.6 μg of Env, 0.2 μg of pcRev, 0.3 μg of pR9ΔEnvΔNef, 0.3 μg of psPAX2-Gag-imCherry, 0.3 μg of YFP-Vpr, and 0.3 μg of either pBJ5-SER2-HA, pBJ5-SER5-HA, or empty pBJ5 vector. Transfection was carried out using JetPrime transfection reagent. Forty eight hours post-transfection, the supernatant was collected and stored at −80 °C. For concentrated viral stock, the viral supernatants were either pelleted through a 20% sucrose cushion by centrifugation at 100,000 × *g* for 2 h at 4 °C or using Lenti-X concentrator (Clontech).

Virus-cell fusion (BlaM), FFWO, and infectivity assays

Virus-cell fusion was measured using the BlaM assay, as described previously (22, 23). Briefly, the target cells were grown in 96-well black clear-bottom plates (Corning) to 95–100% confluency. Viruses (equal amounts of p24) were bound to target cells by centrifugation at 4 °C for 30 min at 1550 × *g* followed by incubation in DMEM without phenol red growth medium at 37 °C, 5% CO_2 for 90 min. The fusion reaction was stopped by placing the plates on ice, and the medium was replaced with the BlaM substrate, CCF4-AM (Invitrogen). Cells were incubated at 12 °C overnight, and the BlaM activity was determined from the ratio of coumarin (blue) and fluorescein (green) fluorescence signals, using a SpectraMaxi3 fluorescence plate reader (Molecular Devices, Sunnyvale, CA). Cell viability was measured using a colorimetric CellTiter Blue assay (Promega) according to the manufacturer's recommendations.

The FFWO assay was carried out using the double-split GFP-luciferase reporter system, as described previously (20). Twenty four hours prior to the experiment, N4X4-DSP-1 and N4X4-DSP-2 cells were seeded at a 1:1 ratio in collagen-coated 96-well black clear-bottom plates (Corning). The confluent co-cultures were preincubated with 40 μM of the cell-permeable *Renilla* luciferase substrate EnduRen™ in HBSS, 10% FBS for 2 h, centrifuged with viruses for 30 min at 4 °C (1550 × *g*) to allow virus binding, and washed once with ice-cold HBSS, 10% FBS. FFWO was initiated by incubation at 37 °C, and the resulting luciferase signal was measured using TopCount NXT reader (Perkin-Elmer Life Sciences). For virus infectivity, the target cells were inoculated with viruses, as described above, and cultured at 37 °C, 5% CO_2 for 24–36 h. The luciferase signal was detected using the Bright-Glo luciferase substrate.

Virus inactivation assay

To assess virus inactivation over time, pseudoviruses (normalized for p24) were suspended in phenol-free growth medium supplemented with 10 mM HEPES and preincubated at 37 °C for 4 h. Virus-cell fusion was then measured by the BlaM assay.

p24 ELISA, immunoprecipitation, and Western blotting

The p24 content of viral stocks was determined by ELISA, as described previously (62). For immunoprecipitation experiments, the extracts of HEK293T/17 producer cells were prepared using RIPA without SDS (50 mM Tris-HCl (pH 7.4), 1% Nonidet P-40, 0.1% sodium deoxycholate, and 150 mM NaCl) buffer with complete protease inhibitors (Roche Applied Science), followed by centrifugation at 1500 × *g* for 5 min to sediment nuclei. Extracts were adjusted to equivalent protein concentrations using the BCA protein assay kit (Thermo Fisher Scientific, Rockford, IL), and equal aliquots were used for Western blotting or immunoprecipitations. For immunoprecipitation, cell lysates were precleared by adsorption onto protein G Plus/protein A-agarose (Calbiochem, Darmstadt, Germany), followed by incubation with mouse anti-HA (BioLegend, San Diego) (1:200 dilution) and subsequent addition of protein G Plus/protein A-agarose. Equal amounts of p24 or total protein were loaded onto 4–15% polyacrylamide gel (Bio-Rad). Proteins were transferred onto a nitrocellulose membrane, blocked with 10% Blotting-grade Blocker (Bio-Rad) for 30 min at room temperature, and incubated with HIV Ig (1:2000 dilution), rabbit anti-HA (Sigma) (1:500 dilution), or mouse anti-α-tubulin (Sigma) (1:3000 dilution). Horseradish peroxidase-conjugated (HRP) goat anti-rabbit antibody (1:500 dilution, Santa Cruz Biotechnology, Dallas, TX), HRP-protein G (1:2000, Bio-Rad), or HRP-rabbit anti-mouse (Millipore) and a chemiluminescence reagent from GE Healthcare were used for protein detection. Precision Plus protein standards (Kaleidoscope™, Bio-Rad) were used as molecular weight markers.

Cell-cell fusion and flow cytometry

For the dual-split protein-based cell-cell fusion assay, 293T-DSP-1 (DSP-1) cells in 100-mm dishes were transfected with 5 μg of pHXB2-Rev (a gift from Dr. Anna Cereseto, University of Trento, Italy) and 5 μg of either pBJ5 (empty vector), pBJ5-SER2-GFP, or pBJ5-SER5-GFP, using JetPrime transfection reagent that was replaced with DMEM after 8 h. Concurrent with 293T-DSP-1 transfection, NP2/CD4/CXCR4/DSP-2 (DSP-2) cells were seeded onto a black wall clear-bottom 96-well plate coated with collagen. Thirty four hours post-transfection, confluent DSP-2 cells were incubated with 60 μM EnduRen^{TM} for 2 h. Next, DSP-1 cells were non-enzymatically dissociated from plates, using Cellstripper^{TM} (Mediatech, Manassas, VA), and 2×10^6 DSP-1 cells were overlaid onto treated DSP-2 in each well. To initiate cell-cell fusion, plates were transferred to 37 °C and incubated for 2 h, after which time the luciferase activity was measured using a TopCount NXT plate reader. In parallel, 4×10^6 cells from each 293T-DSP-1 transfection were cooled on ice and resuspended in ice-cold PBS, 15% FBS for 2 h. Half of each sample was resuspended in 5 μg/ml 2G12 and the other half in PBS (control) and incubated overnight at 4 °C. The following day, all samples were washed three times in ice-cold PBS, resuspended in 2 μg/ml goat anti-human Alexa-647 (Life Technologies, Inc., and Thermo Fisher Scientific, Waltham, MA), incubated on ice for 2 h, and washed three times in ice-cold PBS. Samples were treated for 5 min with propidium iodide solution (Sigma), and single cell propidium iodide, GFP, and Alexa-647 fluorescence were detected using a BD LSR II flow cytometer (BD Biosciences).

Single virus immunofluorescence staining and analyses

Immobilized particle immunofluorescence experiments were performed on pseudoparticles diluted in ice-cold PBS^{++}, filtered through a 0.2-μm filter, and allowed to attach onto poly-L-lysine-coated 8-well chamber slides (Lab-Tek, Nalge Nunc International, Penfield, NY) for 30 min at 4 °C. Wells were washed with cold PBS^{++} to remove unbound virus. Samples were blocked for 2 h at room temperature in PBS^{++}, 15% FBS before addition of 5 μg/ml 2G12 or 2 μg/ml 4E10 with or without 10 μg/ml sCD4 and incubated for 1 h at 37 °C. Samples were washed with PBS^{++}, fixed in 2% fresh paraformaldehyde for 20 min at room temperature, and blocked for 30 min at room temperature in PBS^{++}, 15% FBS before incubation with 2 μg/ml goat anti-human Alexa-647 for 1 h at room temperature. Samples were washed three times with PBS^{++} and imaged immediately or stored at 4 °C for imaging the following day. Stained virus samples were imaged with a Zeiss LSM780 using a Plan-Apo ×63/1.4NA oil-immersion objective in a single Z-plane at 6.3-μs pixel dwell time (for each sample 10–25 fields were imaged containing >1000 particles). GFP, mCherry, and Alexa-647 were excited at 488, 561, and 633 nm, respectively. After acquisition, virus particles were identified as mCherry+ spots using the spot detector algorithm in Volocity. Intensities in GFP, mCherry, and Alexa-647 channels corresponding to two-pixel dilation around mCherry+ spots were background subtracted. Particles were filtered by mCherry intensity to exclude the bottom and top 10% of particles. Using thresholds derived from negative controls, the remaining particles were identified as GFP+ and/or Alexa-647+. The median value was used to parameterize the single particle staining intensity distributions.

Live cell single virus imaging

Single viral fusion experiments were performed with CV1.CD4.CXCR4 cells plated on collagen-coated glass-bottom dishes (MatTek, Ashland, MA) in FluoroBrite DMEM and grown to 70% confluency. Before imaging, the cells were chilled on ice, washed with ice-cold PBS^{++}, and spinoculated with freshly thawed pseudovirus at 4 °C for 20 min at 1500 × *g*. After spinoculation, cells were washed with ice-cold PBS^{++} to remove unbound virus. Virus entry was initiated by addition of pre-warmed live cell imaging buffer. Images were acquired in a single axial plane with a Personal DeltaVision imaging system (Applied Precision, GE Healthcare) using a UPlanFluo ×40/1.3 NA oil objective (Olympus, Tokyo, Japan) and a GFP/Cherry standard filter set (Chroma, Bellows Falls, VT). Two-channel fluorescence emission was recorded in series by an EM-CCD camera (Photometrics, Tucson, AZ) for a single field-of-view imaged every 3 s. During time-lapse imaging, an environmental chamber was used to maintain samples at 37 °C and high humidity, and the UltimateFocus module (Applied Precision, GE Healthcare) was used to compensate for axial drift.

Event annotation, curve fitting, and single particle tracking

Single particle color change (content release) events were annotated using the region of interest manager in ImageJ (National Institutes of Health). Annotated particles were tracked in Volocity (PerkinElmer Life Sciences). The local background subtraction at each time point was performed, using a custom script that created a region of interest encompassing a particle by one- or two-pixel dilation of the tracked object, as described previously (63). A script in Microsoft Excel was designed to collate the tracking data, combining the tracked particle and the dilated object to correct for the local background at each time point.

FRAP

CV-1 cells were seeded onto collagen-coated glass-bottom dishes in FB, grown to 40–50% confluency, and transfected with 100 μl of mixture consisting of 1 μg of either CCR5-GFP or SER5-GFP plasmid and 2 μl of JetPrime transfection reagent, added directly to the microwell. Eight hours post-transfection, the transfection mix was removed, and 2 ml of pre-warmed FB was added to the dishes. Twenty four hours post-transfection, the samples were cooled to room temperature and washed with PBS^{++}. Bleaching and single plane time series imaging at room temperature were acquired with a Zeiss LSM780 using a C-Apo ×40/1.2NA water-immersion objective. Circular regions 2.5 or 4 μm in diameter near the periphery of flat GFP+ cells were photobleached. Fluorescence recovery in the photobleached region was monitored, along with intensity in nearby identically shaped regions, both on and off the cells, to control for inadvertent photobleaching and background signal, respectively. FRAP traces corrected for photobleaching and background were fit to a single-exponential rise-to-maximum curve to

extract the half-time ($t_{½}$) and immobile fraction. Diffusion coefficient was estimated as $D = 0.25 \cdot r^2/t_{½}$ (64), where r is the radius of the bleached region.

Statistical analyses

Unless stated otherwise, statistical analysis was performed using the Student's *t* test or non-parametric Man-Whitney test, as appropriate. Triplicate data for each independent experiment (usually 2–3 experiments) performed under identical conditions were normalized to the internal control and pooled to calculate the mean and standard error. Statistical comparison of dose-response curves for the fusion inhibitors for the control and SER5 viruses was done using the sum of squares reduction test. *, $p < 0.05$; **, $p < 0.01$; ***, $p < 0.001$, *N.S.*, not significant.

Author contributions—C. S. and M. M. designed, performed, and analyzed the experiments and co-wrote the paper. A. C. and M. P. constructed and tested pertinent expression vectors and co-wrote the manuscript. G. B. M. conceived and coordinated the study, analyzed the results, and wrote the paper. All authors reviewed the results and approved the final version of the manuscript.

Acknowledgments—We are grateful to AIDS Research and Reference Reagent Program (National Institutes of Health) for reagents and to the Emory Pediatrics Flow Cytometry and Biostatistics cores (Dr. Courtney McCracken and Scott Gillespie) for help with statistical analyses. We also thank Caleb Mason for excellent technical assistance and members of the Melikyan laboratory for critical reading of the manuscript.

References

1. Aiken, C., and Trono, D. (1995) Nef stimulates human immunodeficiency virus type 1 proviral DNA synthesis. *J. Virol.* **69,** 5048–5056
2. Schwartz, O., Maréchal, V., Danos, O., and Heard, J. M. (1995) Human immunodeficiency virus type 1 Nef increases the efficiency of reverse transcription in the infected cell. *J. Virol.* **69,** 4053–4059
3. Day, J. R., Münk, C., and Guatelli, J. C. (2004) The membrane-proximal tyrosine-based sorting signal of human immunodeficiency virus type 1 gp41 is required for optimal viral infectivity. *J. Virol.* **78,** 1069–1079
4. Cavrois, M., Neidleman, J., Yonemoto, W., Fenard, D., and Greene, W. C. (2004) HIV-1 virion fusion assay: uncoating not required and no effect of Nef on fusion. *Virology* **328,** 36–44
5. Campbell, E. M., Nunez, R., and Hope, T. J. (2004) Disruption of the actin cytoskeleton can complement the ability of Nef to enhance human immunodeficiency virus type 1 infectivity. *J. Virol.* **78,** 5745–5755
6. Tobiume, M., Lineberger, J. E., Lundquist, C. A., Miller, M. D., and Aiken, C. (2003) Nef does not affect the efficiency of human immunodeficiency virus type 1 fusion with target cells. *J. Virol.* **77,** 10645–10650
7. Schaeffer, E., Geleziunas, R., and Greene, W. C. (2001) Human immunodeficiency virus type 1 Nef functions at the level of virus entry by enhancing cytoplasmic delivery of virions. *J. Virol.* **75,** 2993–3000
8. Chowers, M. Y., Spina, C. A., Kwoh, T. J., Fitch, N. J., Richman, D. D., and Guatelli, J. C. (1994) Optimal infectivity *in vitro* of human immunodeficiency virus type 1 requires an intact nef gene. *J. Virol.* **68,** 2906–2914
9. Tobiume, M., Tokunaga, K., Kiyokawa, E., Takahoko, M., Mochizuki, N., Tatsumi, M., and Matsuda, M. (2001) Requirement of nef for HIV-1 infectivity is biased by the expression levels of Env in the virus-producing cells and CD4 in the target cells. *Arch. Virol.* **146,** 1739–1751
10. Rosa, A., Chande, A., Ziglio, S., De Sanctis, V., Bertorelli, R., Goh, S. L., McCauley, S. M., Nowosielska, A., Antonarakis, S. E., Luban, J., Santoni, F. A., and Pizzato, M. (2015) HIV-1 Nef promotes infection by excluding SERINC5 from virion incorporation. *Nature* **526,** 212–217
11. Usami, Y., Wu, Y., and Göttlinger, H. G. (2015) SERINC3 and SERINC5 restrict HIV-1 infectivity and are counteracted by Nef. *Nature* **526,** 218–223
12. Heigele, A., Kmiec, D., Regensburger, K., Langer, S., Peiffer, L., Stürzel, C. M., Sauter, D., Peeters, M., Pizzato, M., Learn, G. H., Hahn, B. H., and Kirchhoff, F. (2016) The potency of Nef-mediated SERINC5 antagonism correlates with the prevalence of primate lentiviruses in the wild. *Cell Host Microbe* **20,** 381–391
13. Inuzuka, M., Hayakawa, M., and Ingi, T. (2005) Serinc, an activity-regulated protein family, incorporates serine into membrane lipid synthesis. *J. Biol. Chem.* **280,** 35776–35783
14. Pizzato, M., Popova, E., and Göttlinger, H. G. (2008) Nef can enhance the infectivity of receptor-pseudotyped human immunodeficiency virus type 1 particles. *J. Virol.* **82,** 10811–10819
15. Ahi, Y. S., Zhang, S., Thappeta, Y., Denman, A., Feizpour, A., Gummuluru, S., Reinhard, B., Muriaux, D., Fivash, M. J., and Rein, A. (2016) Functional interplay between murine leukemia virus glycogag, Serinc5, and surface glycoprotein governs virus entry, with opposite effects on gammaretroviral and ebolavirus glycoproteins. *mBio* **7,** e01985–16
16. Beitari, S., Ding, S., Pan, Q., Finzi, A., and Liang, C. (2017) Effect of HIV-1 Env on SERINC5 antagonism. *J. Virol.* **91,** e02214–16
17. Trautz, B., Pierini, V., Wombacher, R., Stolp, B., Chase, A. J., Pizzato, M., and Fackler, O. T. (2016) The antagonism of HIV-1 Nef to SERINC5 particle infectivity restriction involves the counteraction of virion-associated pools of the restriction factor. *J. Virol.* **90,** 10915–10927
18. Usami, Y., and Göttlinger, H. (2013) HIV-1 Nef responsiveness is determined by Env variable regions involved in trimer association and correlates with neutralization sensitivity. *Cell Rep.* **5,** 802–812
19. Clavel, F., and Charneau, P. (1994) Fusion from without directed by human immunodeficiency virus particles. *J. Virol.* **68,** 1179–1185
20. Kondo, N., Marin, M., Kim, J. H., Desai, T. M., and Melikyan, G. B. (2015) Distinct requirements for HIV-cell fusion and HIV-mediated cell-cell fusion. *J. Biol. Chem.* **290,** 6558–6573
21. Wang, J., Kondo, N., Long, Y., Iwamoto, A., and Matsuda, Z. (2009) Monitoring of HIV-1 envelope-mediated membrane fusion using modified split green fluorescent proteins. *J. Virol. Methods* **161,** 216–222
22. de la Vega, M., Marin, M., Kondo, N., Miyauchi, K., Kim, Y., Epand, R. F., Epand, R. M., and Melikyan, G. B. (2011) Inhibition of HIV-1 endocytosis allows lipid mixing at the plasma membrane, but not complete fusion. *Retrovirology* **8,** 99
23. Miyauchi, K., Kim, Y., Latinovic, O., Morozov, V., and Melikyan, G. B. (2009) HIV enters cells via endocytosis and dynamin-dependent fusion with endosomes. *Cell* **137,** 433–444
24. Daecke, J., Fackler, O. T., Dittmar, M. T., and Kräusslich, H. G. (2005) Involvement of clathrin-mediated endocytosis in human immunodeficiency virus type 1 entry. *J. Virol.* **79,** 1581–1594
25. Chernomordik, L. V., and Kozlov, M. M. (2005) Membrane hemifusion: crossing a chasm in two leaps. *Cell* **123,** 375–382
26. Melikyan, G. B., Brener, S. A., Ok, D. C., and Cohen, F. S. (1997) Inner but not outer membrane leaflets control the transition from glycosylphosphatidylinositol-anchored influenza hemagglutinin-induced hemifusion to full fusion. *J. Cell Biol.* **136,** 995–1005
27. Jeetendra, E., Robison, C. S., Albritton, L. M., and Whitt, M. A. (2002) The membrane-proximal domain of vesicular stomatitis virus G protein functions as a membrane fusion potentiator and can induce hemifusion. *J. Virol.* **76,** 12300–12311
28. Padilla-Parra, S., Marin, M., Gahlaut, N., Suter, R., Kondo, N., and Melikyan, G. B. (2013) Fusion of mature HIV-1 particles leads to complete release of a Gag-GFP-based content marker and raises the intraviral pH. *PLoS One* **8,** e71002
29. de Rosny, E., Vassell, R., Jiang, S., Kunert, R., and Weiss, C. D. (2004) Binding of the 2F5 monoclonal antibody to native and fusion-intermediate forms of human immunodeficiency virus type 1 gp41: implications for fusion-inducing conformational changes. *J. Virol.* **78,** 2627–2631
30. Dimitrov, A. S., Jacobs, A., Finnegan, C. M., Stiegler, G., Katinger, H., and Blumenthal, R. (2007) Exposure of the membrane-proximal external region of HIV-1 gp41 in the course of HIV-1 envelope glycoprotein-mediated fusion. *Biochemistry* **46,** 1398–1401

31. Peachman, K. K., Wieczorek, L., Polonis, V. R., Alving, C. R., and Rao, M. (2010) The effect of sCD4 on the binding and accessibility of HIV-1 gp41 MPER epitopes to human monoclonal antibodies. *Virology* **408,** 213–223
32. Melikyan, G. B., Markosyan, R. M., Hemmati, H., Delmedico, M. K., Lambert, D. M., and Cohen, F. S. (2000) Evidence that the transition of HIV-1 gp41 into a six-helix bundle, not the bundle configuration, induces membrane fusion. *J. Cell Biol.* **151,** 413–423
33. Nelson, J. D., Kinkead, H., Brunel, F. M., Leaman, D., Jensen, R., Louis, J. M., Maruyama, T., Bewley, C. A., Bowdish, K., Clore, G. M., Dawson, P. E., Frederickson, S., Mage, R. G., Richman, D. D., Burton, D. R., and Zwick, M. B. (2008) Antibody elicited against the gp41 N-heptad repeat (NHR) coiled-coil can neutralize HIV-1 with modest potency but non-neutralizing antibodies also bind to NHR mimetics. *Virology* **377,** 170–183
34. Lai, R. P., Yan, J., Heeney, J., McClure, M. O., Göttlinger, H., Luban, J., and Pizzato, M. (2011) Nef decreases HIV-1 sensitivity to neutralizing antibodies that target the membrane-proximal external region of TMgp41. *PLoS Pathog.* **7,** e1002442
35. Trkola, A., Purtscher, M., Muster, T., Ballaun, C., Buchacher, A., Sullivan, N., Srinivasan, K., Sodroski, J., Moore, J. P., and Katinger, H. (1996) Human monoclonal antibody 2G12 defines a distinctive neutralization epitope on the gp120 glycoprotein of human immunodeficiency virus type 1. *J. Virol.* **70,** 1100–1108
36. Sanders, R. W., Venturi, M., Schiffner, L., Kalyanaraman, R., Katinger, H., Lloyd, K. O., Kwong, P. D., and Moore, J. P. (2002) The mannose-dependent epitope for neutralizing antibody 2G12 on human immunodeficiency virus type 1 glycoprotein gp120. *J. Virol.* **76,** 7293–7305
37. Rathinakumar, R., Dutta, M., Zhu, P., Johnson, W. E., and Roux, K. H. (2012) Binding of anti-membrane-proximal gp41 monoclonal antibodies to CD4-liganded and -unliganded human immunodeficiency virus type 1 and simian immunodeficiency virus virions. *J. Virol.* **86,** 1820–1831
38. Chan, D. C., Chutkowski, C. T., and Kim, P. S. (1998) Evidence that a prominent cavity in the coiled coil of HIV type 1 gp41 is an attractive drug target. *Proc. Natl. Acad. Sci. U.S.A.* **95,** 15613–15617
39. Demirkhanyan, L., Marin, M., Lu, W., and Melikyan, G. B. (2013) Subinhibitory concentrations of human α-defensin potentiate neutralizing antibodies against HIV-1 gp41 pre-hairpin intermediates in the presence of serum. *PLoS Pathog.* **9,** e1003431
40. Miyauchi, K., Kozlov, M. M., and Melikyan, G. B. (2009) Early steps of HIV-1 fusion define the sensitivity to inhibitory peptides that block 6-helix bundle formation. *PLoS Pathog.* **5,** e1000585
41. Gustchina, E., Hummer, G., Bewley, C. A., and Clore, G. M. (2005) Differential inhibition of HIV-1 and SIV envelope-mediated cell fusion by C34 peptides derived from the C-terminal heptad repeat of gp41 from diverse strains of HIV-1, HIV-2, and SIV. *J. Med. Chem.* **48,** 3036–3044
42. Gustchina, E., Louis, J. M., Bewley, C. A., and Clore, G. M. (2006) Synergistic inhibition of HIV-1 envelope-mediated membrane fusion by inhibitors targeting the N and C-terminal heptad repeats of gp41. *J. Mol. Biol.* **364,** 283–289
43. Steger, H. K., and Root, M. J. (2006) Kinetic dependence to HIV-1 entry inhibition. *J. Biol. Chem.* **281,** 25813–25821
44. Reeves, J. D., Gallo, S. A., Ahmad, N., Miamidian, J. L., Harvey, P. E., Sharron, M., Pohlmann, S., Sfakianos, J. N., Derdeyn, C. A., Blumenthal, R., Hunter, E., and Doms, R. W. (2002) Sensitivity of HIV-1 to entry inhibitors correlates with envelope/coreceptor affinity, receptor density, and fusion kinetics. *Proc. Natl. Acad. Sci. U.S.A.* **99,** 16249–16254
45. Agrawal, N., Leaman, D. P., Rowcliffe, E., Kinkead, H., Nohria, R., Akagi, J., Bauer, K., Du, S. X., Whalen, R. G., Burton, D. R., and Zwick, M. B. (2011) Functional stability of unliganded envelope glycoprotein spikes among isolates of human immunodeficiency virus type 1 (HIV-1). *PLoS One* **6,** e21339
46. Munro, J. B., Gorman, J., Ma, X., Zhou, Z., Arthos, J., Burton, D. R., Koff, W. C., Courter, J. R., Smith, A. B., 3rd., Kwong, P. D., Blanchard, S. C., and Mothes, W. (2014) Conformational dynamics of single HIV-1 envelope trimers on the surface of native virions. *Science* **346,** 759–763
47. Haim, H., Strack, B., Kassa, A., Madani, N., Wang, L., Courter, J. R., Princiotto, A., McGee, K., Pacheco, B., Seaman, M. S., Smith, A. B., 3rd., and Sodroski, J. (2011) Contribution of intrinsic reactivity of the HIV-1 envelope glycoproteins to CD4-independent infection and global inhibitor sensitivity. *PLoS Pathog.* **7,** e1002101
48. Brandenberg, O. F., Magnus, C., Rusert, P., Regoes, R. R., and Trkola, A. (2015) Different infectivity of HIV-1 strains is linked to number of envelope trimers required for entry. *PLoS Pathog.* **11,** e1004595
49. Chernomordik, L. V., and Kozlov, M. M. (2003) Protein-lipid interplay in fusion and fission of biological membranes. *Annu. Rev. Biochem.* **72,** 175–207
50. Cohen, F. S., and Melikyan, G. B. (2004) The energetics of membrane fusion from binding, through hemifusion, pore formation, and pore enlargement. *J. Membr. Biol.* **199,** 1–14
51. Haynes, B. F., Fleming, J., St Clair, E. W., Katinger, H., Stiegler, G., Kunert, R., Robinson, J., Scearce, R. M., Plonk, K., Staats, H. F., Ortel, T. L., Liao, H. X., and Alam, S. M. (2005) Cardiolipin polyspecific autoreactivity in two broadly neutralizing HIV-1 antibodies. *Science* **308,** 1906–1908
52. Wei, X., Decker, J. M., Liu, H., Zhang, Z., Arani, R. B., Kilby, J. M., Saag, M. S., Wu, X., Shaw, G. M., and Kappes, J. C. (2002) Emergence of resistant human immunodeficiency virus type 1 in patients receiving fusion inhibitor (T-20) monotherapy. *Antimicrob. Agents Chemother.* **46,** 1896–1905
53. Li, Y., Svehla, K., Mathy, N. L., Voss, G., Mascola, J. R., and Wyatt, R. (2006) Characterization of antibody responses elicited by human immunodeficiency virus type 1 primary isolate trimeric and monomeric envelope glycoproteins in selected adjuvants. *J. Virol.* **80,** 1414–1426
54. Gao, F., Morrison, S. G., Robertson, D. L., Thornton, C. L., Craig, S., Karlsson, G., Sodroski, J., Morgado, M., Galvao-Castro, B., von Briesen, H., Beddows, S., Weber, J., Sharp, P. M., Shaw, G. M., and Hahn, B. H. (1996) Molecular cloning and analysis of functional envelope genes from human immunodeficiency virus type 1 sequence subtypes A through G. The WHO and NIAID Networks for HIV isolation and characterization. *J. Virol.* **70,** 1651–1667
55. Malim, M. H., Hauber, J., Fenrick, R., and Cullen, B. R. (1988) Immunodeficiency virus rev trans-activator modulates the expression of the viral regulatory genes. *Nature* **335,** 181–183
56. Walker, L. M., Phogat, S. K., Chan-Hui, P. Y., Wagner, D., Phung, P., Goss, J. L., Wrin, T., Simek, M. D., Fling, S., Mitcham, J. L., Lehrman, J. K., Priddy, F. H., Olsen, O. A., Frey, S. M., Hammond, P. W., *et al.* (2009) Broad and potent neutralizing antibodies from an African donor reveal a new HIV-1 vaccine target. *Science* **326,** 285–289
57. Thali, M., Moore, J. P., Furman, C., Charles, M., Ho, D. D., Robinson, J., and Sodroski, J. (1993) Characterization of conserved human immunodeficiency virus type 1 gp120 neutralization epitopes exposed upon gp120-CD4 binding. *J. Virol.* **67,** 3978–3988
58. Stiegler, G., Kunert, R., Purtscher, M., Wolbank, S., Voglauer, R., Steindl, F., and Katinger, H. (2001) A potent cross-clade neutralizing human monoclonal antibody against a novel epitope on gp41 of human immunodeficiency virus type 1. *AIDS Res. Hum. Retroviruses* **17,** 1757–1765
59. Mascola, J. R., Lewis, M. G., Stiegler, G., Harris, D., VanCott, T. C., Hayes, D., Louder, M. K., Brown, C. R., Sapan, C. V., Frankel, S. S., Lu, Y., Robb, M. L., Katinger, H., and Birx, D. L. (1999) Protection of macaques against pathogenic simian/human immunodeficiency virus 89.6PD by passive transfer of neutralizing antibodies. *J. Virol.* **73,** 4009–4018
60. Desai, T. M., Marin, M., Sood, C., Shi, J., Nawaz, F., Aiken, C., and Melikyan, G. B. (2015) Fluorescent protein-tagged Vpr dissociates from HIV-1 core after viral fusion and rapidly enters the cell nucleus. *Retrovirology* **12,** 88
61. Miyauchi, K., Marin, M., and Melikyan, G. B. (2011) Visualization of retrovirus uptake and delivery into acidic endosomes. *Biochem. J.* **434,** 559–569
62. Kondo, N., and Melikyan, G. B. (2012) Intercellular adhesion molecule 1 promotes HIV-1 attachment but not fusion to target cells. *PLoS one* **7,** e44827
63. Sood, C., Marin, M., Mason, C. S., and Melikyan, G. B. (2016) Visualization of content release from cell surface-attached single HIV-1 particles carrying an extra-viral fluorescent pH-sensor. *PLoS One* **11,** e0148944
64. Kang, M., Day, C. A., Kenworthy, A. K., and DiBenedetto, E. (2012) Simplified equation to extract diffusion coefficients from confocal FRAP data. *Traffic* **13,** 1589–1600